Nair, Manish, Wang, Junyuan, Leiba, Yigal, Zhu, Huiling, Gomes, Nathan J. and Wang, Jiangzhou (2018) *Exploiting Low Complexity Beam Allocation in Multi-User Switched Beam Millimeter Wave Systems.* IEEE Access, 7 . pp. 2894-2903.

Exploiting Low Complexity Beam Allocation in Multi-User Switched Beam Millimeter Wave Systems

Manish Nair[1], Junyuan Wang[2], Yigal Leiba[3], Huiling Zhu[1], Member, IEEE, Nathan J. Gomes[1], Senior Member, IEEE, and Jiangzhou Wang[1], Fellow, IEEE

[1]Communications Research Group, University of Kent, Canterbury CT2 7NT, U.K.
[2]Department of Computer Science, Edge Hill University, Ormskirk, L39 4QP, U.K.
[3]Siklu Communication Ltd, 43 HaSivim St. Petach Tikva 4959501, Israel.

Corresponding author: Manish Nair (e-mail: mn307@kent.ac.uk).

ABSTRACT Switched-beam systems offer a promising solution for realizing multi-user communications at millimeter wave (mmWave) frequencies. A low-complexity beam allocation (LBA) algorithm has been proposed to solve the challenging problem of maximizing sum data-rates. However, there are practical limitations in mmWave systems, such as restrictions in the number of available radio frequency (RF) transceiver chains at the base station (BS), sensitivity to sidelobe interference and the beam generation techniques. In this paper, using generalized beam-patterns, we present the maximum sum data-rates achievable in switched-beam mmWave systems compared to fixed-beam systems by applying LBA. Then, the impact on maximum sum data rates of actual beam-patterns, obtained from a practical mmWave lens antenna, which have higher and non-uniform sidelobes compared to the theoretical beams, is assessed. Finally, as a guide for practical wireless system design, benchmarks are established for relative sidelobe levels that provide acceptable sum data-rate performance when considering generalized beam patterns.

INDEX TERMS Beamforming, beam-allocation, fixed-beam, millimeter wave, mobile communications.

I. INTRODUCTION

The demand for ever higher data-rates along with the scarcity of spectrum in current cellular bands is leading to the adoption of millimeter-wave (mmWave) bands in new generations of cellular networks [1],[2]. The short mmWave wavelength, combined with advances in analog integrated circuit design and radio frequency (RF) semiconductor technology, has enabled the realization of beamforming hardware in which highly directive antenna arrays with small form factors are integrated with compact RF transceiver modules [3],[4]. Beamforming is crucial for facilitating high data-rate transmission at mmWave frequencies to overcome high propagation loss [5],[6].

In multi-user mmWave systems, adaptive-beam and switched-beam based beamforming have been investigated [7],[8]. In adaptive beamforming, sophisticated codebook-based signal processing algorithms are utilized for generating beamforming weights at the base station (BS), which are continuously adjusted to simultaneously generate and steer

several directional beams towards the respective mobile users [9],[10]. However, such a strategy requires obtaining and continual updating of the direction-of-arrival (DoA) of signals from all mobile users, along with full channel state information (CSI). Furthermore, the generation and update of the beamforming codebook involves computationally intensive matrix operations such as a pseudo-inverse [11]. [12] proposes a codebook of beamforming vectors over an initial beam alignment phase, followed by a learning phase where each mobile user estimates the "top-*P*" beams, and reports the beam indices as well as the received signal-to-interference plus noise ratios (SINR) to the BS. However, such an approach can incur considerable feedback overhead between the mobile users and the BS. In [13], a combination of generalized eigenvector codebook and SINR based codeword selection metric with limited feedback is shown to lead to improved ergodic sum data-rates. However, this cannot be adopted into switched beam based beamforming systems. This is because, by contrast, switched-beam based beamforming systems have

to choose from one of several predefined directional spatial beams within a cell in order to enhance the received SINR at the mobile user [5]. The BS determines the beam that is best aligned to the user signal's DoA, and switches to that beam to communicate with the user. The cell is sectorized by many narrow beams with each beam serving an individual user or a group of users. The spatially separated directional beams lead not just to an increase in the possible reuse of frequency channels by reducing potential inter-beam-interference, but also to an increase in transmission range [14],[15]. A particular limitation in switched-beam systems is the frequent hand-offs when the user moves from the sector of one beam to another, as the flexibility of continuous steering is not provided [16]. Although codebook based beamforming systems [11]–[13] have addressed the hand-off issue by beam-training and beam-alignment, however, as indicated earlier, they cannot be directly adopted into switched-beam systems. Moreover, in mmWave systems, the beams have narrow beamwidths, and together with a large number of predefined beams, codebooks cause very high frequency hand-off having a huge signaling overhead. Nevertheless, despite these disadvantages, the switched-beam approach is economically expedient, easy to deploy and maintain (than the completely adaptive systems), thus simplifying practical hardware design.

In switched-beam scenarios where the number of possible beams N is much larger than the number of users K, the low complexity beam allocation (LBA) algorithm, proposed in [17], offers a low computational complexity beam-user search approach to what could be a significant algorithmic problem of maximizing sum data-rates [18]–[21]. For example, the simplest greedy algorithm in [21] has a complexity of $O(KN^2)$, which is too high when the number of beams is large. By contrast, LBA algorithm attains nearly the same sum-data rate as compared to an optimal brute-force search based beam allocation, albeit with a much lower complexity of $O(K \log N)$. In LBA, only those beams with the highest user directivity, known as active beams, are selected for data transmission, and then, to maximize sum data rate, only those users which have the highest receive SINR are selected. The remaining users are discarded and the unselected beams are turned off, focusing transmit power only onto the selected beams/users, and reducing inter-beam interference through having fewer beams. However, in [17], practical limitations, including the number of available RF chains and higher and non-uniform sidelobe levels, were not considered.

In this paper, after describing application scenarios for switched-beam mmWave systems in Section II, we apply LBA to a switched-beam mmWave system with a limited number of RF chains. In Section III, we develop generalized, theoretical beam patterns based on element fed arrays, having an idealized main lobe with fixed beam gain and angular resolution, along with exponentially decaying sidelobes [22]. Using these theoretical beam patterns, we show the performance benefit of switched-beam systems, using the LBA, over comparable fixed-beam mmWave systems, which are practically simple but constantly generate fixed numbers of beams. Fixed-beam networks along with beam selection has emerged as a popular technique in hybrid analog-digital beamforming systems due to its simplicity [23]–[26]. By applying this fixed-beam network in hybrid analog-digital beamforming systems, a number of analog beams are first selected (which produce a high array gain) and a digital beamformer is then adopted based on the selected analog beams [27]–[30]. The design of the digital beamformer serves to attain certain objective functions such as maximization of sum capacity, minimization of SINR, optimization of energy efficiency etc. However, digital beamformer design entails sparse mmWave channel estimation along with (at least) partial channel feedback, again incurring feedback and signaling overhead [27]–[30]. LBA avoids these whilst achieving near optimal sum data-rates, subject to saturation due to inter-beam interference at higher transmit powers. Subsequently, in Section IV, we use measured beam patterns of a practical lens antenna system, to show that improved performance can be obtained despite high and non-uniform sidelobe levels. Finally, in Section V, we determine the level of sidelobe interference that can be tolerated before system performance is degraded to the level of a fixed beam system, thereby providing guidance for future antenna and wireless system designers. The paper is concluded in Section VI.
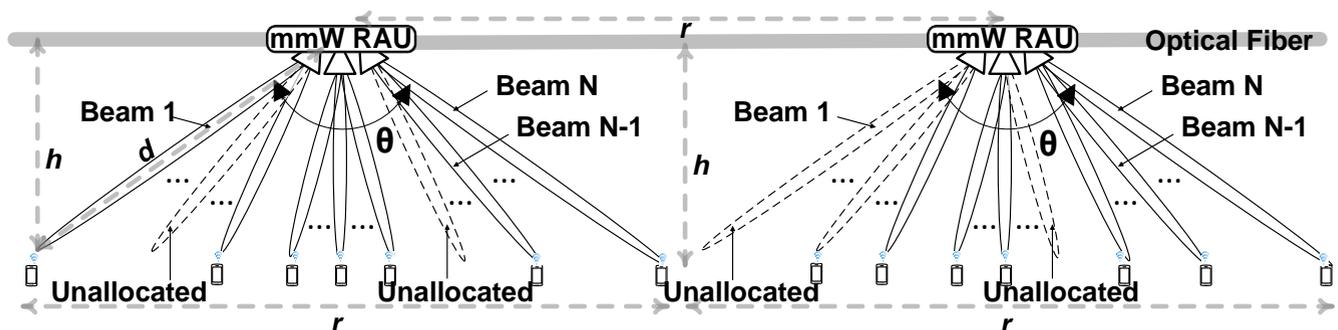

FIGURE 1. Application scenario showing ceiling mounted mmWave RAUs generating N beams communicating simultaneously with different mobile users. The inter-RAU distance r depends on the angle of coverage θ and height h of the mmWave RAU.

II. APPLICATION SCENARIO DESCRIPTION

TABLE I

Variation of Angle of Coverage θ and inter-RAU distance d of mobile users with height h of ceiling mounted RAU.

mmWave RAU Ceiling Mount Height: $h = 5$m		
$\theta = 15°$	$r \approx 1.4$m	$d \approx 5$m
$\theta = 45°$	$r \approx 3.8$m	$d \approx 5.4$m
$\theta = 120°$	$r \approx 10.6$m	$d \approx 10$m
mmWave RAU Ceiling Mount Height: $h = 10$m		
$\theta = 15°$	$r \approx 2.6$m	$d \approx 10$m
$\theta = 45°$	$r \approx 7.7$m	$d \approx 10.8$m
$\theta = 120°$	$r \approx 17.3$m	$d \approx 20$m
mmWave RAU Ceiling Mount Height: $h = 20$m		
$\theta = 15°$	$r \approx 5.2$m	$d \approx 20.2$m
$\theta = 45°$	$r \approx 15.3$m	$d \approx 21.6$m
$\theta = 120°$	$r \approx 36.6$m	$d \approx 40$m

The switched-beam mmWave system in Fig. 1 shows remote antenna units (RAUs) [31],[32], which might be mounted on a ceiling, capable of generating beams in N distinct directions. Several ceiling mounted RAUs can be connected by optical fiber, as indicated in Fig.1, and coordinated by a central BS unit (not shown in the figure). Each beam is able to transmit independent data-streams, and every RAU can serve multiple mobile users simultaneously. Assuming that there are generally no obstacles between RAUs and users, ceiling mounted RAUs communicate with users by line-of-sight (LoS) communication. In our paper, although application scenario is restricted to LoS, it could be easily extended for non-line-of-sight (NLoS) as well. An analysis of NLoS transmission at mmWave would have to apply the modified Saleh-Valenzuela (SV) channel with clustered ray multi-path propagation as investigated in [27]. The AoDs would then correspond to the dominant ray multi-path cluster of the mmWave channel, not the initial beam AoD from the RAU. Moreover, in a mmWave channel, it is the LoS path that is dominant, and the NLoS paths are weak due to the high propagation loss, scattering and blockage in mmWave environments. Nevertheless, this work is generalizable for NLoS cases also. The inter-RAU distance, denoted by r, is the distance between two successive ceiling mounted RAUs providing contiguous coverage. For the system to provide geographical coverage, the inter-RAU distance will depend on the height of the ceiling mount h, here assumed to be the minimum user-antenna distance, the overall coverage angle of the beams denoted by θ, and the maximum user-antenna distance, denoted by d in Fig. 1. The dependence of inter-RAU distance r on h, d and θ can be derived based on the simple geometric relationships: $\tan(\theta/2) = r/2h$, and $\cos(\theta/2) = h/d$. Examples are provided in Table I. From Table I, it can be observed that for narrower coverage angles θ and larger ceiling mount heights h, the maximum and minimum user-RAU distances d are similar to the ceiling mount height h.

This assumption of constant distance $h \approx d$ is applied later in the paper.

In a switched-beam system, the angular coverage of each beam is generally much less than the angular coverage of the RAU. Moreover, coverage is generally non-contiguous as only beams with users currently in their coverage would be switched on. In the RAU, RF chains are needed for each beam that is switched on. Thus, in a real system, the number of RF chains present in a RAU limits the number of beams that can be simultaneously switched on. By contrast, a fixed beam system needs to provide complete angular coverage for the RAU. For a fixed beam system with the same number of RF chains as the switched beam system, the beams would be less directional. In the extreme case, a single beam system employs a much less directional beam, with much lower antenna gain, but requires only one RF chain.

III. SERVING MULTIPLE USERS WITH LIMITED RF CHAINS

A downlink model of a switched-beam mmWave system is considered. Denote $\mathcal{K}$ as the set of users and $\mathcal{N}$ as the set of available beams, where $|\mathcal{K}| = K$ and $|\mathcal{N}| = N$. It is assumed that a limited number of RF chains can select a certain number of beams from the set of N available beams in order to serve up to N_{RF} users. It is also assumed every RF chain is fed by independent data-streams. Hence, $N_{RF} \leq K \leq N$. Beam-allocation and user-selection are decided by the two-step, low complexity beam allocation (LBA) algorithm [17].

A. LOW-COMPLEXITY BEAM ALLOCATION (LBA) ALGORITHM

The LBA algorithm consists of beam-user association and user-selection.

Beam-user association: In the beam-user association step, each user k is associated with the beam n_k^* which has the largest directivity at the k-th user, given by

$$n_k^* = \underset{n \in \mathcal{N}}{\operatorname{argmax}}\, D_n(\theta_k), \text{for all } k. \tag{1}$$

where $D_n(\theta_k)$ is the beam-directivity of the k-th user associated with the n-th beam and located at θ_k.

User selection: Based on the assumption that a limited number of RF chains, it is imperative to select users from the set of associated users for each beam. The set of associated users for beam n is defined as

$$\mathcal{K}_n^* = \{k | n_k^* = n, \text{for all } k\}. \tag{2}$$

Let $\mathcal{N}_a^*$ denote the set of all the associated beams. The user selection step is then given by

$$k^* = \underset{k \in \mathcal{K}_n^*}{\operatorname{argmax}}\, D_n(\theta_k), \text{for all } n \in \mathcal{N}_a^*. \tag{3}$$

In the user-selection step, only one user which has the highest directivity is selected from the set of associated users

$\mathcal{N}_n^*$ for the n-th beam, where $n \in \mathcal{N}_a^*$. This process is repeated for every associated beam and results in the highest sum data rate.

In [17], for the LBA algorithm, there was no limit to the number of possible beams and there could be as many as required according to the number of users. In this work, when the further limitation of number of RF chains is added, a selection is made of the best N_{RF} beams from the set of associated beams $\mathcal{N}_a^*$ obtained in the beam-user association step of the LBA. After the beam-user association and user-selection steps, any unallocated beams are turned off by turning off the associated RF chains, and any unselected users are discarded. Let $\mathcal{N}^*$ be the final set of allocated beams, and $\mathcal{K}^*$ denote the set of served users, respectively. Assuming that the total transmit power of the switched-beam mmWave system is fixed at P and is equally allocated among active beams, the transmit power allocated to any active beam n is given by

$$P_n = \begin{cases} \dfrac{P}{N^*}, & n \in \mathcal{N}^*, \\ 0, & n \notin \mathcal{N}^*. \end{cases} \quad (4)$$

Since the number of users that can be served is limited by the number of RF chains, $K^* \leq N_{RF}$. The assumption of a limited number of RF chains was made in order to obtain the sum data-rate in a practical switched-beam mmWave system. A single beam could serve multiple users through common multiple access techniques, e.g., time division multiple access (TDMA), orthogonal frequency division multiple access (OFDMA), or, non-orthogonal multiple access (NOMA) [33]. The principle of NOMA can effectively double the number of served users, keeping the number of RF chains constant. In NOMA, each allocated beam $\mathcal{N}^*$ and the associated RF chain can serve two users instead of one. The two served users are known as the strong-user and the weak-user, respectively. Strong-user selection can proceed as explained in (3). Denote this selected strong-user as k_s^*. Having selected the strong user, the selection of the weak-user pair can be given by

$$k_w^* = \underset{k \in \mathcal{K}_n^* \setminus k_s^*}{\arg\min} D_n(\theta_k), \text{for all } n \in \mathcal{N}_a^*. \quad (5)$$

In the weak user selection step, only that user which has the least directivity is selected from the set of associated users $\mathcal{N}_n^*$ for the n-th beam, where $n \in \mathcal{N}_a^*$. This is because the selection of two served users per beam results in intra-beam interference from the strong user k_s^*, experienced by its weak-user pair k_w^*. The LBA algorithm can be suitably modified to apply the principle of NOMA. However, such an investigation has been left for a future work.

Sum data-rate calculation: The SINR for the k-th user which is served by the n_k^*-th beam is given by

$$\text{SINR}_{k,n_k^*}$$
$$= \frac{P_n D_{n_k^*}(\theta_k) L(\rho_k)}{\mathcal{F}_k + \kappa\tau B + \Sigma_{l \in N^*, l \neq n_k^*} P_l D_l(\theta_k) L(\rho_k)}, \text{for all } k \quad (6)$$
$$\in \mathcal{K}^*$$

where $\mathcal{F}_k$ is the cascaded noise power of the mmWave receiver components at the k-th user and $\kappa\tau B$ is the thermal noise power at the user for the mmWave downlink system. $L(\rho_k) = (4\pi\rho_k f_c/c)^{-2}$ is the LoS path loss, $f_c = 60\text{GHz}$ is the mmWave operating frequency, $\rho_k=10\text{m}$ is the distance of the k-th user from the antenna elements (RAU), and $c = 3 \times 10^8 \text{m/s}$ is the velocity of electromagnetic radiation in free space. The sum data-rate is given by

$$R_s = \sum_{k \in \mathcal{K}^*} \log_2\big(1 + \text{SINR}_{k,n_k^*}\big). \quad (7)$$

It is expected that in the high transmit power regime, inter-beam interference, represented by the summation term in the denominator of (6), will also be high, causing the sum data-rates to saturate.

User Scheduling and SINR Constraints: In switched beam systems, since the beams are predefined (as the set of available beams $\mathcal{N}$), the beam-user association step can be accomplished simultaneously for the set of available beams $\mathcal{N}$ within a single time-slot. User selection step can also be accommodated within the same time-slot.

LBA already accounts for SINR constraints because, (i) each user can only be associated with one beam (Equation (1)), and, (ii) an associated beam only select one user (Equation (3)). Although these constraints avoid severe inter-beam interference and enhances the received SINR, the scheduled/selected users will nonetheless experience
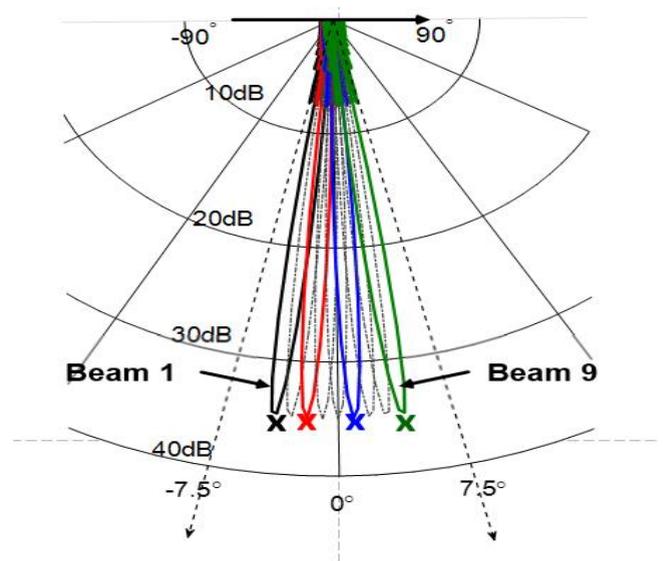

FIGURE 2. An example switched-beam mmW system having up to 9 idealized beams in one plane and a set of 4 users in that plane, each user represented by the "x".

interference from the beams that are allocated to other users, because of which the sum data-rates saturate.

Sum Data-Rate and User Fairness: Since LBA maximizes the sum-data rate, not all users can be simultaneously served. The application of LBA to a practical switched-beam mmWave system with limited number of RF chain hence produces an upper bound for the sum-data rate performance in such systems. To ensure fairness among users with varying locations, individual data rate constraints for users can be added into the sum data rate maximization problem, which would be carefully investigated in our future work.

B. SWITCHED-BEAM AND FIXED BEAM COVERAGE

Fig. 2 illustrates an example switched-beam mmWave system, in one plane of operation, where $N = 9$ potential beams provide a coverage of $-7.5° \leq \theta \leq 7.5°$, meaning that each beam has a coverage approximately equal to $1.6°$. It is assumed that there are $N_{RF} = 4$ RF chains, so up to $N^* = 4$ beams out of the potential set of $N = 9$ beams can be selected by implementing LBA. Thus, the system (in this plane) can provide coverage for up to $K = 4$ users, assuming that a beam is allocated to each user. If 2 users (out of the $K = 4$) are associated to the same beam, then in the user selection step of LBA, only the user with the higher directivity, as defined in (3) is selected, while the other is discarded. Hence, only 3 users are served in

such a case. The switched-beam system is benchmarked against a fixed-beam system, with two cases considered.

1) Fixed-Beam: All Beams On

Here, the set of beams providing contiguous coverage are always active, i.e. $N^* = N$. The beams are equivalent to sectors in a standard antenna system. A greedy algorithm can be implemented, whereby for the set of N beams and K users, beams are allocated to users greedily, based on the achievable SINR, to maximize sum data rate. This can be mathematically represented as

$$(k^*, n_k^*) = \underset{k \in \mathcal{K}, n_k \in \mathcal{N}}{\arg\max} \, \text{SINR}_{k, n_k}. \tag{8}$$

2) Fixed-Beam: Unallocated Beams Off

In this case, there is an additional step that if there are no users in the coverage area of a beam, it is switched off and the power is reallocated to other beams. The maximum sum data-rate for the fixed-beam systems is then derived as previously in (7). In reality, in both switched-beam and fixed-beam systems, fairness, for example by sharing beams, may be taken into account, but this would not give the maximum sum data-rate.

To benchmark the switched-beam system with $N_{RF} = 4$ RF chains, the fixed-beam system is assumed to have $N = 4$ beams over the same coverage range, hence requiring each beam to have a beam width of $\approx 3.75°$. A beam gain of 35dB

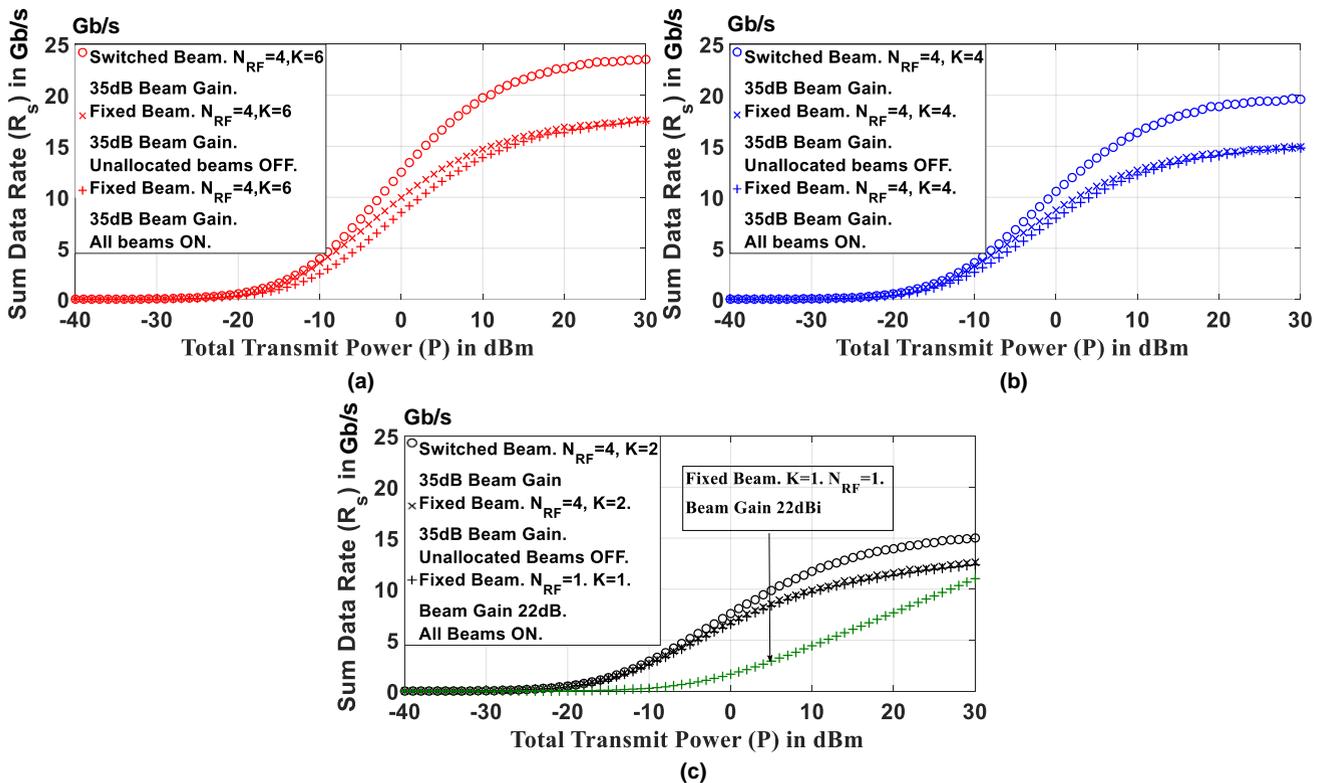**FIGURE 3.** Estimated sum data-rates in b/s for switched-beam and the two adaptations of fixed-beam mmWave systems, for (a) K=6 (red), (b) K=4 (blue), and (c) K=2 (black) as well as K=1 (green) user scenarios. There are N_RF=4 RF chains able to transmit independent data-streams through up to 4 active beams. Center frequency f_c=60GHz, system bandwidth B=1GHz. The distance of the users from the antenna elements is 10m.

is assumed, as high as in the switched-beam system, as technologically it is likely to be easier to manufacture high gain fixed antennas [34]. As a further comparison, a system with a single beam covering the angular range $-7.5° \leq \theta \leq 7.5°$ can be considered. An antenna for such a system (when a standard gain horn) is likely to have a gain of 22dB [35].

C. SUM DATA-RATES WITH IDEALIZED BEAMS

In this subsection, the estimated sum data-rates of the switched-beam and fixed-beam mmWave systems with idealized beam patterns are compared for different cases.

The estimated sum data-rates vs. total system transmit power for 10,000 realizations of uniformly distributed mobile user locations are shown in Fig. 3 (a), (b), and (c), for $K = 6$, $K = 4$ and $K = 2$ users, respectively, for a bandwidth $B = 1$GHz. Although both switched-beam and fixed-beam systems have the same beam gain of 35dB, the switched-beam achieves higher estimated sum-data rates. This is because: (i) there are more potential beams for the switched-beam system giving a higher likelihood that the user is nearer a maximum gain angle of a beam, and, (ii) there will generally be higher inter-beam interference in the fixed-beam system. Low transmit power data-rates are limited by thermal noise, while the saturation at high powers is caused by the inter-beam interference. When unallocated beams are turned off, there is a small improvement in the average fixed-beam performance at lower transmit powers. This is because there occurs an improvement in the received SINRs when the unallocated beams are turned off. However at higher transmit
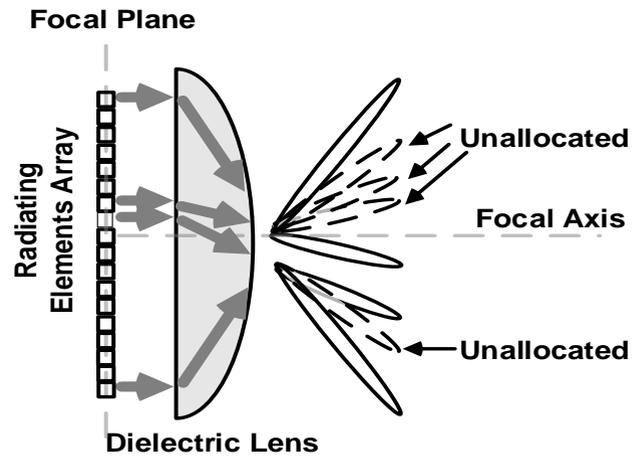

FIGURE 4. Schematic diagram illustrating the concept of SIKLU lens antenna.

powers, the inter-beam interference (which saturates the sum data-rates) dominates over any improvement in the received SINR (observed at lower transmit powers with unallocated beams turned off). This results in similar saturated sum data-performance in both the fixed-beam cases.

Comparing the cases for different number of users in the coverage plane, it can be seen that the switched-beam case shows increasingly enhanced performance for more users, as the users that are allocated beams are more likely to be at positions with high beam gain. On the other hand, as the maximum sum data-rate is being calculated, the assumption
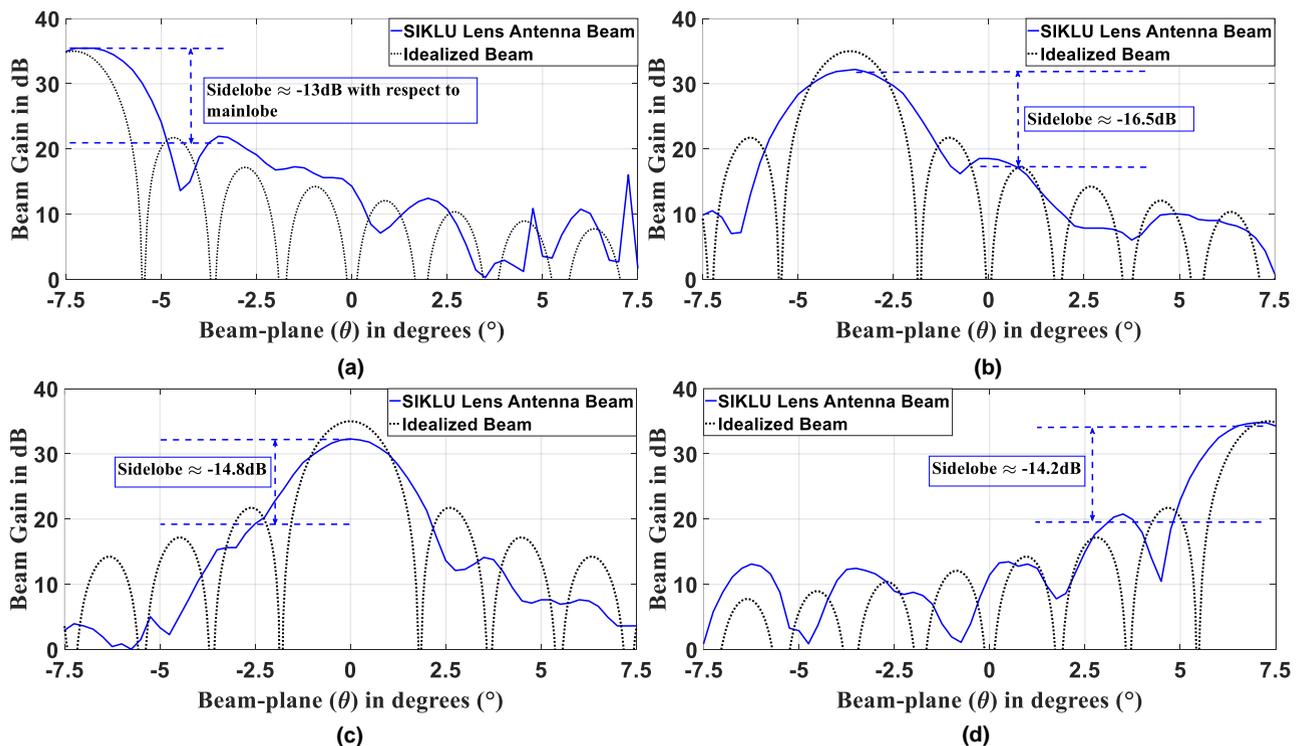

FIGURE 5. Measured beam patterns from 4 of the radiating elements in a SIKLU lens antenna, overlaid with 4 idealized beams. (a) Overlay of SIKLU lens antenna beam and idealized beam at $\theta = -7.5°$, (b) Overlay at at $\theta = -1.25°$, (c) at $\theta = 0°$, and (d) $\theta = +7.5°$.
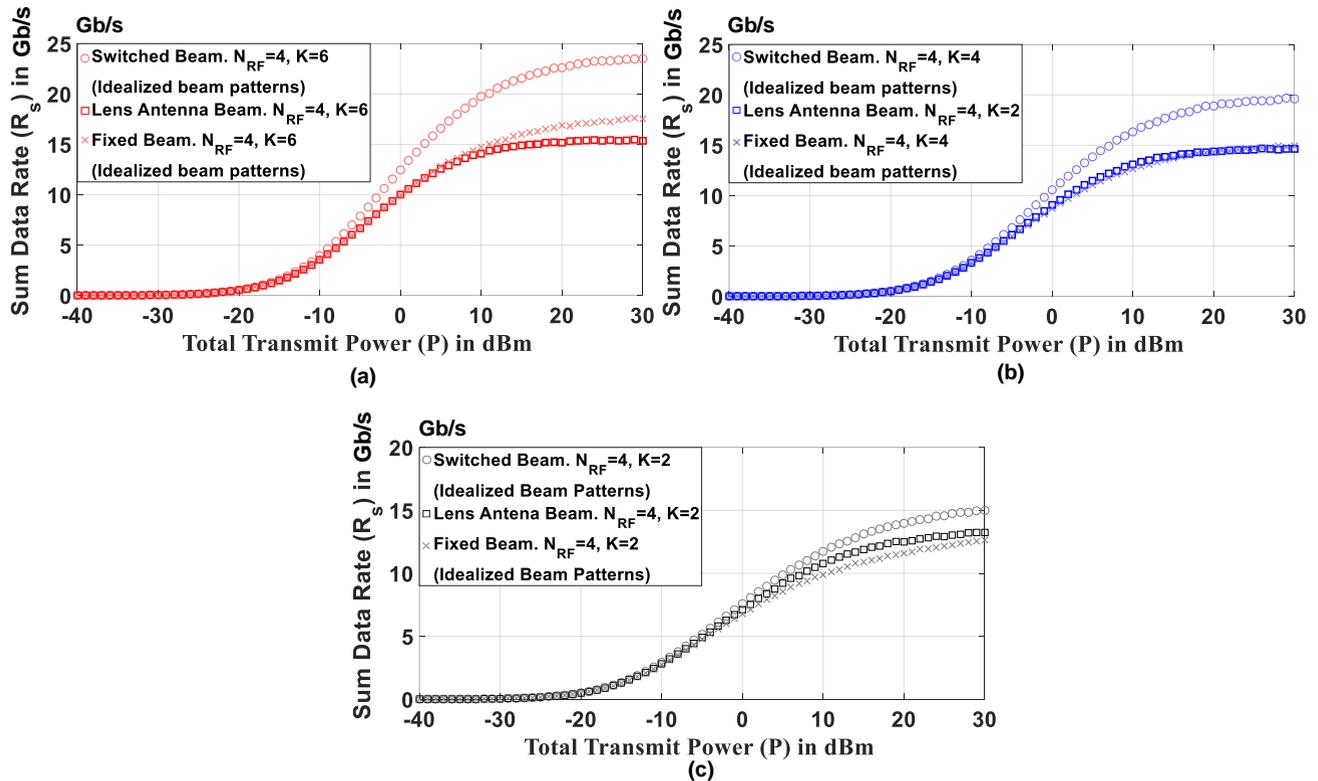
FIGURE 6. mmWave sum data-rates for SIKLU lens antenna switched-beam system: (a) $K = 6$ user scenario, (b) $K = 4$ user scenario, and, (c) $K = 2$ user case. Also shown for comparison are the idealized switched-beam and fixed-beam results as presented in Fig.3. The fixed-beam system corresponds to the adaptation when all beams are active.

is that in all cases, there may be users who are not served, increasingly so for larger numbers of users (an investigation including fairness is left for future work).

Finally, Fig. 3(c) shows the sum data-rate when only a single beam of 22dB gain provides coverage for the whole angular range; as expected, much reduced sum data-rates at reasonable power levels are observed. This system is not limited by inter-beam interference, at least not by beams from the same RAU.

IV. mmWAVE BEAM GENERATION WITH LENS ANTENNA

A research and development (R&D) prototype lens antenna is considered as a practical example of a mmWave switched-beam system [36]. Fig. 4 illustrates its principle of operation; it is constituted by a convex dielectric lens and radiating antenna elements arrayed on its focal plane. A switching matrix would enable the selection of beams out of the total number available, with a requirement for RF chains in order to distribute different signals using the selected beams. The number of beams available is defined by the number of radiating elements. A lens antenna avoids phase shifting of each radiating element as would be required by an array antenna.

Fig. 5. shows overlaid measured beam patterns from 4 radiating elements in the SIKLU lens-antenna with 4 beams from the switched-beam system model that were generated in MATLAB for the results of Section III. Fig. 5(a) and Fig.

5(d) represent the extreme edges of coverage, where as Fig. 5(b) and Fig. 5(c) represent those nearer the center. It can be observed that the beam angles are well aligned to each other, and the mainlobe beam gain levels are closely matched. However, the practical lens antenna produces generally higher and non-uniform sidelobes. The high sidelobe measurements in the lens antenna can attributed to: (i) any unevenness in the density of the glass lens, (ii) surface smoothness of the fabricated lens, (iii) any impedance mismatch between the passive radiating elements array (Fig. 4) mounted on a printed circuit board (not shown in the figure) and the respective RF chain, or, (iii) system integration issues. Lastly, these measurements were conducted on the very first R&D prototype, and improvements can be expected in the later prototypes.

The simulations performed in Section III were repeated, this time using the measured beam patterns. The results in Fig. 6. demonstrate the impact of the higher and non-uniform sidelobes on the achievable sum data rates. As before, results in Fig. 6(a), Fig. 6(b) and Fig. 6(c) are for the $K = 6$, $K = 4$ and $K = 2$ user scenarios, respectively. It is observed that the data-rate performance of the lens-antenna switched-beam system (with the SIKLU lens-antenna beams) has reduced to approximately that of the fixed-beam system. It should be noted that the fixed-beam system is idealized, of course, and practical antennas will exhibit at least some non-uniformity. The higher sidelobes in the lens-antenna (Fig. 5) cause a

general reduction in the saturated (interference-limited) sum data-rate performance in the lens-antenna switched-beam system as compared to the idealized switched-beam system (Fig. 6). While the received signal power at the user is proportional only to the directivity of the mainlobe of the allocated beam (see SINR Equation (6)), high sidelobes add to the received interference power at the user (not the received signal power). Lower mainlobe gain in the lens-antenna system are also a factor.

In [37], the Taylor-synthesis method was applied to 2x2 uniformly-fed subarrays of a 16x16 slot antenna array to design an efficient amplitude tapering antenna-feed network, which provided amplitude and phase control for selecting specific sidelobe levels. A similar approach could be incorporated into the design of future R&D prototypes of the SIKLU lens-antenna array for attaining sidelobe reduction. The effect of high sidelobe interference in the saturated sum-data rate performance is investigated in detail in the next Section. Lastly, inter-beam interference becomes significant for increased numbers of users as there will typically be more beams switched on.

V. SIDELOBE INTERFERENCE IMPACT ON SUM DATA-RATES

In the previous section, it was observed that high sidelobe interference in the SIKLU lens antenna beams resulted in a reduction in sum data-rates for a switched-beam system. In this section, the reduction in sum data-rates in a switched-beam system is calibrated against the sidelobe level for idealized beam-patterns based on element-fed linear arrays, which can be considered as a generalized discrete spatial Fourier transform [38]. These result in exponentially decaying sidelobes, as shown in Fig. 7(a).

The sidelobe level is defined as ratio of the first sidelobe to mainlobe, as shown in Fig. 7(a). In this investigation, the sidelobe level is decremented from -13.5dB to -9.5dB in steps of 1dB for the total transmit power levels of 0dBm, 10dBm and 30dBm. The sum data-rates are obtained for $K = 6$, $K = 4$ and $K = 2$ users. The results are shown in Figs. 7(b)-(d). In general, it can be observed that as the relative sidelobe level increases, higher interference causes the sum data-rates of the switched-beam system to fall, eventually to below that of the fixed-beam systems, which are shown in Figs. 7(b)-(d) as benchmarks for their respective user scenarios.

Fig. 7(b) shows that for a system with 0dBm total transmit power, in order to provide improved performance, the sidelobe level in a multi-user switched-beam mmWave system should be lower than -10dB in the $K = 6$ user case. For $K = 2$ users, the required sidelobe level reduces to -11dB. Fig. 7(c) shows that for total transmit power of 10dBm, improved performance is obtained for sidelobe levels lower than -9.5dB for $K = 6$ users. It reduces to approximately -9.8dB and -10.5dB for $K =$
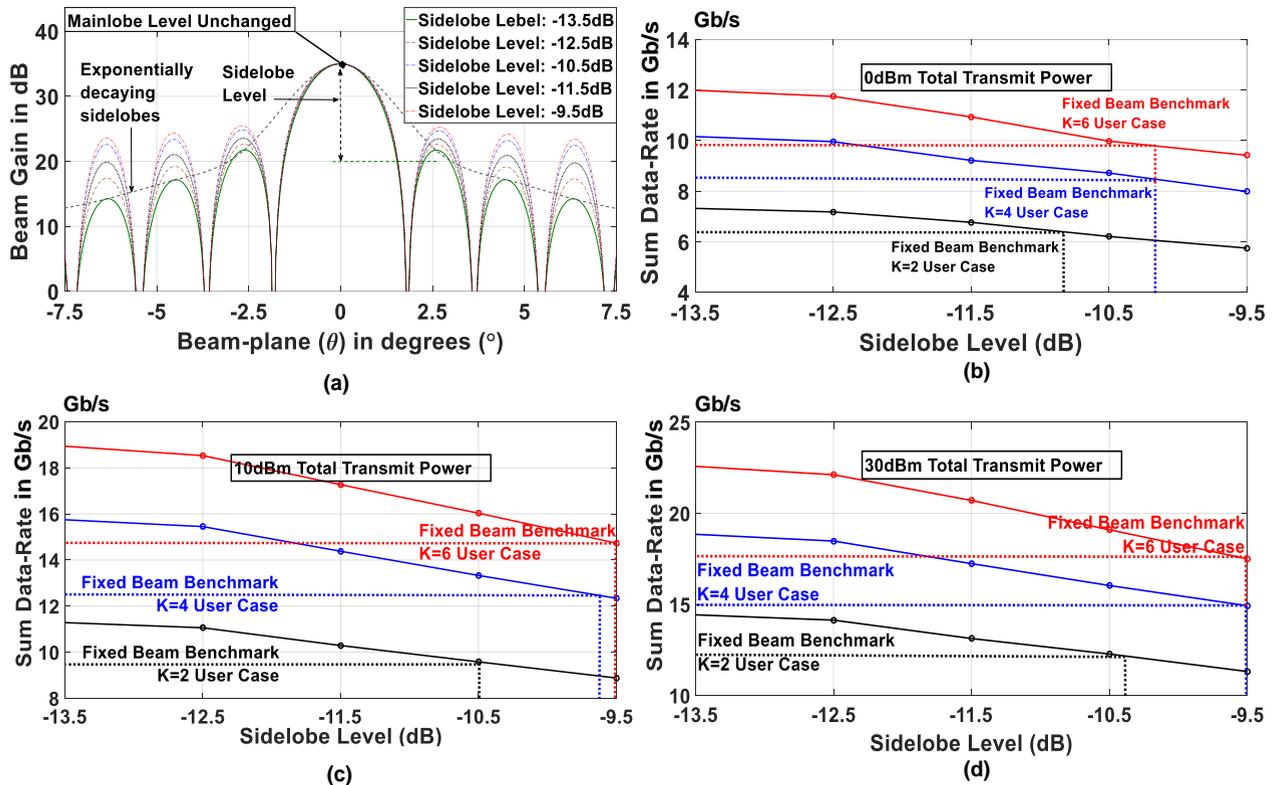

FIGURE 7. mmWave sum data-rates for varying sidelobe levels. (a) Beam pattern indicating exponentially decaying sidelobe levels. Different relative sidelobe levels are simulated for fixed transmit powers, (b) Sum data-rates vs. change in relative sidelobe level for 0dBm total transmit power, (c) for 10dBm total transmit power, and, (c) for 30dBm total transmit power.

4 and $K = 2$ users respectively. The results are similar in Fig. 7(d) for the total transmit power level of 30dBm, except for $K = 2$ users for which the benchmark is at approximately -10.3dB.

In general, the sum data-rate for $K = 2$ falls to the fixed-beam benchmark at lower sidelobe levels than for $K = 4$ or $K = 6$. This occurs because as the number of users decreases when the number of possible beams remains the same, the received power per user increases, improving the received SINR. Hence, $K = 2$ user is more robust to sidelobe interference. Based on these observations, it can be inferred that multi-user switched-beam mmWave systems are sensitive to sidelobe interference. The results in Fig. 7 therefore provide guidance to antenna system engineers for beam pattern requirements in multi-user switched beam mmWave systems.

VI. CONCLUSIONS

In this paper, the maximum sum data-rate performance of a multi-user switched-beam mmWave system with a limited number of RF chains has been studied. The LBA has been applied to both theoretical and practical beam patterns (the latter for a lens-antenna) and benchmarked against an ideal fixed-beam mmWave system. Simulation results show that the switched-beam system outperforms the fixed-beam system in mmWave systems. The sensitivity of switched-beam performance to relative sidelobe level was investigated. Guidance for the required sidelobe level suppression for generalized antenna beam patterns has been given for systems that will employ switched-beams.

ACKNOWLEDGMENT

REFERENCES

[1] M. Dohler, C.M. Chen, R. Q. Hu, R. Annaswamy, M. Simsek, D. Wang, A. Dutta, P. Nikolich and I. Seskar, "IEEE 5G and Beyond: Technology Roadmap White Paper", October 2017.

[2] C. Jiannong et.al., "5G New Radio: Standards and Technology", *ZTE Communications*, vol. 15, no. S1, June 2017.

[3] W. Choi, K. Park, Y. Kim, K. Kim and Y. Kwon, "A V-Band Switched Beam-Forming Antenna Module Using Absorptive Switch Integrated With 4X4Butler Matrix in 0.13um CMOS," *IEEE Transactions on Microwave Theory and Techniques,* vol. 58, pp. 4052-4059, 2010.

[4] J. Moghaddasi and K. Wu, "Millimeter-Wave Multifunction Multiport Interferometric Receiver for Future Wireless Systems," *IEEE Transactions on Microwave Theory and Techniques,* vol. PP, pp. 1-15, 2017.

[5] C. E. Patterson, W. T. Khan, G. E. Ponchak, G. S. May and J. Papapolymerou, "A 60-GHz Active Receiving Switched-Beam Antenna Array With Integrated Butler Matrix and GaAs Amplifiers," *IEEE Transactions on Microwave Theory and Techniques,* vol. 60, pp. 3599-3607, 2012.

[6] J. Ala-Laurinaho, J. Aurinsalo, A. Karttunen, M. Kaunisto, A. Lamminen, J. Nurmiharju, A. V. Räisänen, J. Säily and P. Wainio, "2-D Beam-Steerable Integrated Lens Antenna System for 5G E-Band Access and Backhaul," *IEEE Transactions on Microwave Theory and Techniques,* vol. 64, pp. 2244-2255, 2016.

[7] T. Nishio, H.-P. Tsai, Y. Wang and T. Itoh, "A high-speed adaptive antenna array with simultaneous multibeam-forming capability," *IEEE Transactions on Microwave Theory and Techniques,* vol. 51, pp. 2483-2494, 2003.

[8] F. F. He, K. Wu, W. Hong, L. Han and X. P. Chen, "Low-Cost 60-GHz Smart Antenna Receiver Subsystem Based on Substrate Integrated Waveguide Technology," *IEEE Transactions on Microwave Theory and Techniques,* vol. 60, pp. 1156-1165, 2012.

[9] S. Farzaneh and A. R. Sebak, "Microwave Sampling Beamformer #x2014;Prototype Verification and Switch Design," IEEE Transactions on Microwave Theory and Techniques, vol. 57, pp. 36-44, 2009.

[10] M. A. Piqueras, G. Grosskopf, B. Vidal, J. Herrera, J. M. Martinez, P. Sanchis, V. Polo, J. L. Corral, A. Marceaux, J. Galiere, J. Lopez, A. Enard, J. L. Valard, O. Parillaud, E. Estebe, N. Vodjdani and Moon-So, "Optically beamformed beam-switched adaptive antennas for fixed and mobile broad-band wireless access networks," IEEE Transactions on Microwave Theory and Techniques, vol. 54, pp. 887-899, 2006.

[11] M. Hawes, L. Mihaylova, F. Septier and S. Godsill, "Bayesian Compressive Sensing Approaches for Direction of Arrival Estimation With Mutual Coupling Effects," IEEE Transactions on Antennas and Propagation, vol. 65, pp. 1357-1368, 2017.

[12] M. R. Castellanos, V. Raghavan, J. H. Ryu, O. H. Koymen, J. Li, D. J. Love and B. Peleato, "Channel-Reconstruction-Based Hybrid Precoding for Millimeter-Wave Multi-User MIMO Systems," IEEE Journal of Selected Topics in Signal Processing, vol. 12, pp. 383-398, 5 2018.

[13] V. Raghavan, J. J. Choi and D. J. Love, "Design Guidelines for Limited Feedback in the Spatially Correlated Broadcast Channel," in *IEEE Transactions on Communications*, vol. 63, no. 7, pp. 2524-2540, July 2015.

[14] K. Hosoya, N. Prasad, K. Ramachandran, N. Orihashi, S. Kishimoto, S. Rangarajan and K. Maruhashi, "Multiple Sector ID Capture (MIDC): A Novel Beamforming Technique for 60-GHz Band Multi-Gbps WLAN/PAN Systems," IEEE Transactions on Antennas and Propagation, vol. 63, pp. 81-96, 2015.

[15] M.-S. Lee, V. Katkovnik and Y.-H. Kim, "Minimax robust M-beamforming for radar array with antenna switching," IEEE Transactions on Antennas and Propagation, vol. 53, pp. 2549-2557, 2005.

[16] S.-K. Yong, P. Xia and A. Valdes-Garcia, 60GHz Technology for Gbps WLAN and WPAN:From Theory to Practice, Wiley Telecom, 2011.

[17] J. Wang, H. Zhu, L. Dai, N. J. Gomes and J. Wang, "Low-Complexity Beam Allocation for Switched-Beam Based Multiuser Massive MIMO Systems," IEEE Transactions on Wireless Communications, vol. 15, pp. 8236-8248, 12 2016.

[18] W. Choi, A. Forenza, J. G. Andrews and R. W. Heath. Jr., "Opportunistic Space-Division Multiple Access With Beam Selection," IEEE Transactions on Communications, vol. 55, pp. 2371-2380, 12 2007.

[19] J. Choi, "Opportunistic beamforming with single beamforming matrix for virtual antenna array," IEEE Trans. Veh. Technol., vol. 60, no. 3, pp. 872–881, Mar. 2011.

[20] M. Xia, Y. C. Wu and S. Aissa, "Non-Orthogonal Opportunistic Beamforming: Performance Analysis and Implementation," IEEE Transactions on Wireless Communications, vol. 11, pp. 1424-1433, 4 2012.

[21] J. L. Vicario, R. Bosisio, C. Anton-Haro, and U. Spagnolini, "Beam selection strategies for orthogonal random beamforming in sparse networks," IEEE Trans. Wireless Commun., vol. 7, no. 9, pp. 3385–3396, Sep. 2008.

[22] D. Bai and S. S. Ghassemzadeh and R. R. Miller and V. Tarokh, "Beam Selection Gain from Butler Matrices", IEEE 68th Vehicular Technology Conference, pp. 1-5, 2008

[23] J. Brady and A. Sayeed, "Beamspace MU-MIMO for High-Density Gigabit Small Cell Access at Millimeter-Wave Frequencies," in Proceedings IEEE SPAWC, pp. 80–84, June 2014.

[24] P. Amadori and C. Masouros, "Low RF-Complexity Millimeter-Wave Beamspace-MIMO Systems by Beam Selection," IEEE Transaction Wireless Communications., vol. 63, no. 6, pp. 2212–2223, June 2015.

[25] J. Hogan and A. Sayeed, "Beam Selection for Performance-Complexity Optimization in High-Dimensional MIMO Systems," in Proceedings CISS, pp. 337–342, Mar. 2016.

[26] X. Gao, L. Dai, Z. Chen, Z. Wang, and Z. Zhang, "Near-Optimal Beam Selection for Beamspace mmWave Masive MIMO systems," IEEE Communication. Letters, vol. 20, no. 5, pp. 1054–1057, May 2016.

[27] O. E. Ayach, S. Rajagopal, S. Abu-Surra, Z. Pi, and R. W. Heath, "Spatially Sparse Precoding in Millimeter Wave MIMO Systems," IEEE Transaction Wireless Communications., vol. 13, no. 3, pp. 1499–1513, Mar. 2014.

[28] A. Alkhateeb, O. E. Ayach, G. Leus, and R. W. Heath, "Channel Estimation and Hybrid Precoding for Millimeter Wave Cellular Systems," IEEE J. Select. Topics Signal Process., vol. 8, no. 5, pp. 831–846, Oct. 2014.

[29] L. Liang, W. Xu, and X. Dong, "Low-Complexity Hybrid Precoding in Massive Multiuser MIMO Systems," IEEE Wireless Communication Letters, vol. 3, no. 6, pp. 653–656, Dec. 2014.

[30] F. Sohrabi and W. Yu, "Hybrid Digital and Analog Beamforming Design for Large-Scale MIMO Systems," in Proc. IEEE ICASSP, pp. 2929–2933, Apr. 2015.

[31] H. Zhu, "Performance Comparison Between Distributed Antenna and Microcellular Systems," IEEE Journal on Selected Areas in Communications, vol. 29, pp. 1151-1163, 6 2011.

[32] J. Wang, H. Zhu and N. J. Gomes, "Distributed Antenna Systems for Mobile Communications in High Speed Trains," IEEE Journal on Selected Areas in Communications, vol. 30, pp. 675-683, 5 2012.

[33] Z. Ding, R. Schober and H. V. Poor, "A General MIMO Framework for NOMA Downlink and Uplink Transmission Based on Signal Alignment," in IEEE Transactions on Wireless Communications, vol. 15, no. 6, pp. 4438-4454, June 2016.

[34] L. Chang, Z. Zhang, Y. Li, S. Wang and Z. Feng, "Air-Filled Long Slot Leaky-Wave Antenna Based on Folded Half-Mode Waveguide Using Silicon Bulk Micromachining Technology for Millimeter-Wave Band," IEEE Transactions on Antennas and Propagation, vol. 65, pp. 3409-3418, 2017.

[35] A. Maltshev et.al., "Channel Models for IEEE 802.11a", IEEE 802.11-15/1150r9, May 2016.

[36] Y. Leiba, D. Dayan, Y. Fein, M. Steeg, A. Stohr, T. Inoue, H. Murata, M. Nair, N.J. Gomes, Y. Yanemoto, M. Szczensy and M. Kosciesza, "Report on Beam Steerable Directive Antennas", EU H2020 Programme Project: RAPID ICT-643297, September 2017 (https://www.researchgate.net/project/Radio-technologies-for-5G-using-Advanced-Photonic-Infrastructure-for-Dense-user-environments-RAPID).

[37] G.L. Huang, S.G. Zhou, T.H Chio, H-T. Hui and T.S. Yeo, "A Low Profile and Low Sidelobe Wideband Slot Antenna Array Feb by an Amplitude-Tapering Waveguide Feed-Network", IEEE Transactions on Antennas and Propagation, Vol. 63, No. 1, January 2015.

[38] J. Wang, H. Zhu and N. J. Gomes, "Distributed Antenna Systems for Mobile Communications in High Speed Trains," IEEE Journal on Selected Areas in Communications, vol. 30, pp. 675-683, 5 2012.

MANISH NAIR received B.E in Electronics and Communications Engineering from Viveswaraya Technological University (VTU), India in 2007 and MS in Electrical Engineering from the University of Texas at Dallas (UTD) in 2010, where he was a Graduate Research Assistant.

From 2009 until 2014, he was associated with Nokia Siemens Networks, Skyworks Solutions Inc., Samsung Telecommunications America and Qualcomm. In December 2014, he joined the University of Kent, Canterbury, U.K, where he is currently pursuing a Ph.D. His research interests include hybrid-beamforming and performance analysis of millimeter-wave wireless communications systems.

JUNYUAN WANG (S'13-M'15) received the B.S. degree in Communications Engineering from Xidian University, Xi'an, China, in 2010, and Ph.D. degree in Electronic Engineering from City University of Hong Kong, Hong Kong, China, in 2015.

Dr. Wang is currently a Lecturer (Assistant Professor) at Edge Hill University, Ormskrik, U.K. She was a Research Associate at the University of Kent, Canterbury, U.K. Her research interests include modelling, performance analysis and optimization of wireless communication systems, with particular interests in distributed antenna systems/C-RAN, massive MIMO, and device-to-device communications.

YIGAL LEIBA holds an MSc Degree in Electrical Engineering from the Technion, Haifa, Israel.

Yigal Leiba is a co-founder and CTO of SIKLU. In previous positions, he worked for Runcom Technologies, in charge of the design and the development of the world's first mobile-WiMAX (802.16e) chip, and a voting member of the IEEE 802.16 standard committee. He was also a co-founder and CTO of Breezecom's LMDS group, a spin-off of Breezecom (today Alvarion (NASDAQ: ALVR)). His career includes project management and chief Engineer positions at Breezecom, where he was responsible for development of wireless access and wireless LAN systems. Before Breezecom, he was an R&D engineer in the Israeli Ministry of Defense Electronics Research Department.

HUILING ZHU (M'04) received the B.S degree from Xidian Univeristy, Xian, China, and the Ph.D. degree from Tsinghua University, Beijing, China. She is currently a Reader (Associate Professor) at the University of Kent, United Kingdom. Her research interests are in the area of wireless communications, covering topics such as radio resource management, distributed antenna systems, MIMO, cooperative communications, device-to-device communications, and small cells and heterogeneous networks. She received the best paper award from IEEE Globecom 2011.

Dr. Zhu has participated in a number of European and industrial projects in these topics. She has served as the Symposium Co-Chair for IEEE Globecom2015 and IEEE ICC 2018. Currently, she serves as an Editor for IEEE Transactions on Vehicular Technology.

NATHAN J. GOMES (M'92–SM'06) received the B.Sc. degree from the University of Sussex, Sussex, U.K., in 1984, and the Ph.D. degree from University College London, London, U.K., in 1988, both in electronic engineering.

From 1988 to 1989, Professor Gomes held a Royal Society European Exchange Fellowship with ENST, Paris, France. Since late 1989, he has been with the University of Kent, Canterbury, U.K., where he is currently Professor of Optical Fibre Communications. Professor Gomes' current research interests include fiber-wireless access, and radio over fiber. Professor Gomes was TPC Chair for IEEE International Conference on Communications, ICC 2015, co-chair for IEEE Intl. Topical Meeting in Microwave Photonics 2014, and Track Chair for Microwave Photonics at Asia-Pacific Photonics conference (APC) 2017.

JIANGZHOU WANG (M'91–S M'94–F'16) is currently the Professor of Telecommunications at the University of Kent, United Kingdom. He is the author of over 200 papers in international journals and conferences in the areas of wireless mobile communications and is the author of three books.

Professor Wang was the Technical Program Chair of the 2013 IEEE WCNC in Shanghai and the Executive Chair of the 2015 IEEE ICC in London. He serves/served as an Editor for a number of international journals such as IEEE Transactions on Communications, IEEE Journal on Selected Areas in Communications. He received the Best Paper Award from 2012 IEEE GLOBECOM. Professor Wang was an IEEE Distinguished Lecturer from 1/2013 to 12/2014. He is an IEEE Fellow and an IET Fellow.

Professor Wang's research interests include wireless multiple access and radio resource allocation techniques, massive MIMO and small-cell technologies, device-to-device communications in cellular networks, and distributed antenna systems.